where

$$S = \frac{f}{C_2\xi}\left\{\xi - 1 \pm \left[(1-\xi)^2 - 2\xi^2 + \frac{2\xi C_2}{f}\frac{MR - C_1}{M_0}\right]^{1/2}\right\} \quad (15)$$

The condition for $S$ to have equal roots is the vanishing of the radical in Eq. (15); thus,

$$f = 2C_2\frac{C_1 - MR}{M_0}\frac{\xi}{2 - (1+\xi)^2} \quad (16)$$

in which the constants $C_2/P_0$, $C_1C_2^2/P_0M_0$, and $C_2^2/P_0M_0$ must be determined from the available experimental data for the pump inducer under consideration. When these constants are properly determined, Eq. (16) becomes

$$f = (1.900 - 0.279\,MR)\,P_i/[2 - (1 + 0.00225\,MRP_i)^2] \quad (17)$$

Assigning values of 4.0, 4.5, 5.0, 5.5, and 6.0 to $MR$, five curves, $f$ vs $P_i$, may be plotted as shown in Fig. 1b. The experimental data for $MR$ = 4.5, 5.0, and 5.5 are also shown in Fig. 1b.

### Conclusions

The analysis contained herein employs a first-order mathematical model, the mechanism of which is dependent on the experimental data observed on the *J*-2 LOX pump inducer under consideration. This semiempirical approach to the present study is deemed necessary, because a general study of a problem of this kind would entail investigations in at least the following disciplines of physical science: gas dynamics, bubble dynamics, cryogenics, vibration, hydrofoil dynamics with full or partial cavitation, etc., and with coupling among various thermal, hydrodynamic, and fluid flow effects. Such a study would be extremely time consuming, if not impossible. On the other hand, guided by the experimental evidence as to the occurrence of instability in a frequency, $f$, vs pump inlet pressure, $P_i$, plot, with the mixture ratio as a parametric constant, a model can be devised having a retarded time ($\alpha f^{-1}$) for the present study. The result is an approximate relationship among the principal variables $P_i$, $f$, and $MR$, which outlines the region of instability or the region of oscillation-prone pump operations.

Two such model studies were undertaken in this report: the first is pump inlet-pressure oriented, the second is mixture ratio oriented. When the resulting curves from both model studies were superimposed on the same frequency vs inlet pressure plot, areas of instability or regions of pressure oscillations corresponding to different values of mixture ratios are clearly indicated. With such a plot available, predictions for occurrence of oscillations in some heretofore unsuspected areas can be made. To rephrase it, some undesirable frequency (mixture ratio combinations which would give rise to pressure oscillations in the pump inducer) can be forecast.

Some mathematical expediency is exercised in solving for the roots of Eq. (5). The resultant saving of computational work can be easily appreciated. However, as a consequence of this approximation, extrapolation beyond $P_i$ = 25 psig (first model) and exceeding $MR$ = 6.0 (second model) is not suggested.

The mixture ratio is a function of the $N$ (rpm) and the flow coefficient ($Q/N$) of the pump, where $Q$ is the volumetric flow rate. With the previously derived marginal stability relationships among $f$, $P_i$, and $MR$, one can extend the usefulness of the formulation by relating the frequency of oscillations to the flow coefficient (angle of attack) and the absolute speed of the pump.

### References

[1] Gross, L. A., "J-2 Engine Test Report," March 1969, NASA.
[2] Churchill, R. V., *Operational Mathematics*, McGraw-Hill, New York, 1958.

# Vehicle Flight Scaling with Aerodynamic Flow Hysteresis

PETER JAFFE*
*Jet Propulsion Laboratory, Pasadena, Calif.*

### Nomenclature

| | | |
|---|---|---|
| $A$ | = | cross-sectional area of body |
| $C_D$ | = | drag coefficient |
| $C_m$ | = | pitching moment coefficient |
| $C_{m_\alpha}$ | = | pitching moment coefficient slope |
| $C_{m_q} + C_{m_{\dot\alpha}}$ | = | dynamic stability coefficient |
| $C_{L_\alpha}$ | = | lift coefficient slope |
| $d$ | = | diameter of body |
| $I$ | = | transverse moment-of-inertia |
| $m$ | = | mass of body |
| $\alpha$ | = | angle of attack |
| $\delta\alpha$ | = | angle-of-attack decay in half cycle |
| $\rho$ | = | atmospheric density |
| $\Omega$ | = | distance frequency of oscillation, rad/ft of travel |

CERTAIN aerodynamic configurations, particularly those with flares, are susceptible to flowfield hysteresis as a result of the oscillatory motion they experience in flight. The consequence of this hysteresis is that the static aerodynamic coefficients are no longer single-valued functions of the angle of attack. Since most free-flight analyses[1,2] assume single-valued functions, there is a question about the correctness of using the coefficients obtained from a test to predict the motion of the actual vehicle when hysteresis is present.

This Note will consider the simplest case: a vehicle oscillating in a plane and experiencing a pitching moment hysteresis. The pitching moment history, as the vehicle oscillates from zero angle of attack to its amplitude $\alpha_0$ and then back to zero again, is shown in Fig. 1. As a result of the hysteresis, the energy associated with each half of the motion is different.

A derivation of the dimensionless angle-of-attack decay $\delta\alpha/\alpha_0$ for this case, using an energy balance method is given in Ref. 3. The lift-slope and drag coefficients are assumed constant and the hysteresis is assumed superimposed on a

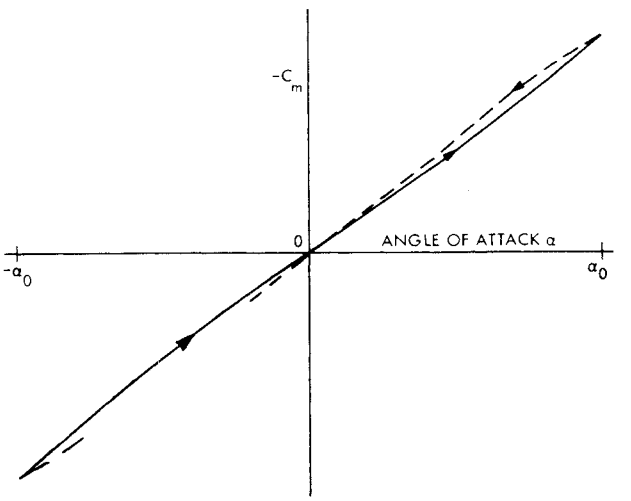


**Fig. 1 Pitching moment coefficient with hysteresis.**

Received September 17, 1969. This paper presents the results of one phase of research carried out at the Jet Propulsion Laboratory, California Institute of Technology, under Contract NAS 7-100, sponsored by NASA.

* Member of the Technical Staff. Member AIAA.

nominally linear pitching moment. Thus,

$$\frac{\delta\alpha}{\alpha_0} = \frac{\pi}{\Omega d}\frac{\rho Ad}{4m}\left[C_{L_\alpha} - C_D - \frac{md^2}{I}(C_{m_q} + C_{m_{\dot\alpha}})\right] - \frac{1}{C_{m_\alpha}\alpha_0^2}\int_{-\alpha_0}^{+\alpha_0} C_m d\alpha \quad (1)$$

The last term in the equation is the contribution due to hysteresis. The real dynamic stability coefficient, given by Eq. (1) when a hysteresis is present, is as follows:

$$(C_{m_q} + C_{m_{\dot\alpha}})_{\text{real}} = -\frac{I}{md^2}\left[\left(\frac{\delta\alpha}{\alpha_0} - \frac{1}{C_{m_\alpha}\alpha_0^2}\int_{-\alpha_0}^{+\alpha_0} C_m d\alpha\right)\frac{\Omega d}{\pi}\frac{4m}{\rho Ad} - C_{L_\alpha} + C_D\right] \quad (2)$$

However, if a test is performed where the presence of a hysteresis is not known, its influence will be lumped into an apparent or test dynamic stability coefficient, which is the sum of the real coefficient and the hysteresis effect:

$$(C_{m_q} + C_{m_{\dot\alpha}})_{\text{apparent}} = (C_{m_q} + C_{m_{\dot\alpha}})_{\text{real}} + \xi$$

where

$$\xi \equiv \left[\frac{\Omega d}{\pi}\frac{4m}{\rho Ad}\frac{I}{md^2}\frac{1}{C_{m_\alpha}\alpha_0^2}\int_{-\alpha_0}^{+\alpha_0} C_m d\alpha\right]_{\text{test hysteresis}} \quad (3)$$

If this apparent coefficient is taken for the real coefficient and used to calculate the decay motion of a different size vehicle or one with a different mass distribution, the following results are obtained from Eq. (1):

$$\left(\frac{\delta\alpha}{\alpha_0}\right) = \frac{\pi}{\Omega d}\frac{\rho Ad}{4m}\left[C_{L_\alpha} - C_D - \frac{md^2}{I}(C_{m_q} + C_{m_{\dot\alpha}})_{\text{real}}\right] - \xi\left(\frac{\pi}{\Omega d}\frac{\rho Ad}{4m}\frac{md^2}{I}\right)_{\text{scaled vehicle}} \quad (4)$$

It is obvious that the predicted decay from this equation is not the same as would be predicted by using the real dynamic stability coefficient in Eq. (1). The difference lies in the quantity $\xi$, which is not necessarily the same for the two cases. However, if the dimensionless frequency $\Omega d$ is the same, then $(\rho Ad/4m)(md^2/I)$, which equals $-[(\Omega d)^2/2C_{m_\alpha}]$, is the same. If, in addition, the oscillatory amplitudes $\alpha_0$ are the same for both cases, then, the scaled and test values of this term will be the same and the decay prediction of the scaled vehicle will be correct.

Although the case considered is simple, it nevertheless points out the fact that, as a minimum requirement for scaling, both the dimensionless frequency and the amplitude must be matched. If the motion is nonplanar, the problem of scaling becomes more complex. For motion that is completely circular, no flow hysteresis will occur, whereas planar motion creates a situation most susceptible to flow hysteresis. It seems obvious that, to match the hysteresis history, the scaled and test bodies must exhibit the same degree of nonplanar motion. For nonplanar motion, therefore, an additional parameter (or parameters) that describe the motion must also be matched for proper scaling. As a final note, one should not forget that, in addition to the motion parameters, the flow parameters, Mach number, Reynolds number, and enthalpy level must also be matched.

### References

[1] Murphy, C. H., "Free-Flight Motion of Symmetric Missiles," Rept. 1216, July 1963, Ballistic Research Lab., Aberdeen Proving Ground, Md.

[2] Nicolaides, J. D., "On the Free-Flight Motion of Missiles Having Slight Asymmetries," Rept. 858, June 1953, Ballistic Research Lab., Aberdeen Proving Ground, Md.

[3] Jaffe, P., "A Generalized Approach to Dynamic-Stability Flight Analysis," TR 32-757, July 1965, Jet Propulsion Lab., Pasadena, Calif.

# Effects of Simulated Degrading Environment on Temperature Control Surfaces

W. D. Miller,* G. L. Brown,† and E. E. Luedke‡
*TRW Systems Group, Redondo Beach, Calif.*

DATA exist concerning most of the recognized effects of 1) prelaunch atmosphere, 2) launch and staging, 3) charged particles in vacuum, and 4) ultraviolet irradiation in vacuum, upon the thermal characteristics of many commonly used materials. The particular design of the INTELSAT III satellite imposed an additional requirement upon the stability of one of its thermal control surfaces. Specifically, the plume radiance from an internally mounted rocket engine, used for synchronous orbit insertion, is such during firing that the adjacent surfaces are raised to a very high temperature for a short period of time. One of these surfaces (the spacecraft end cover) is then exposed to the ultraviolet and charged particle irradiation during the remainder of the spacecraft life. The temperature of this end cover is a function of its solar absorptance. In order to complete the thermal analysis of the spacecraft, it was necessary to determine the solar absorptance and emittance of this surface as a function of this sequence of events. It was also necessary to determine the plume absorptance of the coating during the motor firing in order to compute the end cover temperature. The heat input, $E$, to a surface by radiation is $E = \alpha G$, where $G$ is the irradiation and $\alpha$ is the fraction absorbed.

The absorptance $\alpha$ may be determined by weighting the spectral absorptance over the spectral irradiance of the source. The power emitted by a surface equals $\epsilon\sigma T^4$. Monochromatically, the emittance of an opaque surface equals the absorptance. Hence, the total emittance can be obtained by weighting the spectral absorptance with the Planckian radiator function for the temperature of the surface. It is theoretically possible to have a surface with very low *solar* absorptance and very high 300°K emittance, as there is practically no spectral overlap of the solar irradiance and the 300°K Planckian radiator function. The same situation does not hold for a low plume absorptance and high emittance, since there is considerable overlap spectrally between the 1820°K plume temperature and 300°K and higher Planckian radiator functions.

There are two types of thermal control surfaces which are exposed to high temperatures during the spacecraft life. The first type, illustrated by the INTELSAT III end cover, is exposed to a high temperature and then must function as a low solar absorptance, high 300°K hemispherical emittance surface in sunlight. The second type operates at high temperature, and only the stability of its emittance at temperature (high or low depending upon the application) is important.

Presented as Paper 69-1024 at the AIAA/ASTM/IES 4th Space Simulation Conference, Los Angeles, Calif., September 8–10, 1969; submitted September 24, 1969; revision received October 30, 1969.

* Member of the Technical Staff.
† Member of the Technical Staff. Associate AIAA.
‡ Head, Thermophysics Section.